IJST, Transactions of Mechanical Engineering, Vol. 38, No. M2, pp 431-438
Printed in The Islamic Republic of Iran, 2014

"Research Note"

EXPERIMENTAL STUDY ON MECHANICAL PROPERTIES AND MICROSTRUCTURES IN A 36 REPAIR BUTT WELDMENT*

A. FADAEI** AND M. H. JOKAR

Dept. of Mechanical Engineering, Engineering Faculty, Bu-Ali Sina University, Hamedan, I. R. of Iran
Email: as.fadaei@gmail.com

Abstract– Welding is one of the usual assembling methods with various applications. The different defects are generated during welding and also in service conditions. After inspection and identifying the defects, the repairs are applied. Welding repair operation causes the mechanical properties and the microstructures of weldment to change. In the present work the variations of yield stress, hardness and microstructures in the A 36 repair butt specimens were investigated by the experimental study. The welding technique was Tungsten Insert Gas method without using filler. The specimens were cut from the welded plates using water jet method for avoiding heat effect during the cutting. The low-carbon steel A 36 thin plate was used to construct the specimens. This material has numerous applications to construct various structures and parts. The specifications of specimens and tests were selected according to the standards. The tensile tests were performed for four numbers of each specimen. The mean of yield stresses in the specimens were reduced after the repairing through half- thickness of the butt welds. Moreover, the mean of yield stresses in the specimens after repairing would be decreased if the welding voltage and current increased. Reduction of the hardness in heat affected zone and variation of the phases and grain size after repairing were other outcomes from testing on the specimens.

Keywords– Experimental tests, repairing weld, gas tungsten arc welding, yield stress, hardness, microstructures

1. INTRODUCTION

Welding is one of the customary assembling methods in industrial production processes. High static strength, lightweight joint and short time of treatment are some advantages of weld joints. Many factors affect the quality and efficiency of the weld such as skill of welder, welding wire material and welding speed and so on. Any violation of welding standard principles causes genesis of defects on the surface and depth of weld; furthermore, in service conditions the weld joints meet defects. Defects play an important role in reducing component life and occurrence of sudden failure. After inspection and identifying the location and depth of defects, repair operations are performed. Welding repair operation may change mechanical properties as the tensile strength and microstructures as percent and distribution of the pearlite phase in weldment.

In the last two decades mechanical properties and microstructures in repair welds have been attractive to researchers. Kanne Jr. et al [1] used metallographic analysis to investigate helium-embrittlement cracking around repair welds in nuclear reactor tanks at the Savannah River Site. The scanning electron microscopy was used to support crack analysis and to show the dimple structure arising on fracture surfaces caused by helium-induced cavity formation along grain boundaries. Ghosh Chowdhury and co-workers [2] analyzed the failure of a weld repaired turbine casing after 30 years of total service, including 5 years after weld repair. The propagation of cracks generated by thermal fatigue was facilitated by the

*Received by the editors October 15, 2012; Accepted April 8, 2014.
**Corresponding author

formation of embrittled σ-phase at the austenite grain boundary and this ultimately led to an early failure of the casing. Kanne Jr. and co-workers [3] developed a model that qualitatively showed the interaction of the variables producing helium embrittlement cracking in maintenance of an accelerator for production of tritium. The conventional repair welding processes produced severe cracking in irradiated stainless steel. The overlay technique provided a potential method for repair or modification of accelerator materials exposed to irradiation. Lant et al. [4] reviewed and appraised the practical weld repair procedures that had been developed or were currently being considered for low alloy ferritic steels used within the power, petrochemical and refinery industries. They showed some conclusions about the expected life of repair welds. Otegui and co-workers [5] evaluated three failures in welded full encirclement sleeve repairs in a 24 in the gas pipeline based on fractographic, metallurgical, mechanical and fracture mechanics analyses. These failures were related to poor manufacturing procedures. Nonaka and co-workers [6] experimentally evaluated the performance of repair welds on power boiler. Thick parts such as header and steam piping were repaired with post-weld heat treatment to clarify the mechanical properties of the repair welded joints. It was proven that the toughness would be restored by repair welding. Qian and Lippold [7] discussed the combined effects of δ-phase, grain size and fraction of special grain boundaries in the context of Heat Affected Zone (HAZ) liquation cracking that occurs during repair welding of wrought alloy 718. The major microstructures were changed resulting from multiple weld repair/post weld heat treatment cycles. Branza et al. [8] developed an automated Tungsten Insert Gas (TIG) technique to weld repair high nickel, high chromium heated resistant alloys based on a complementary approach, including thermal instrumentation, numerical simulation and metallurgical investigation. Klobčar et al. [9] developed the model that was applied to predict deformation and detect areas critical to cracking at repair-welding of complex-geometry tooling. They determined a relationship between the welding parameters and characteristic weld dimensions, to select the most appropriate geometry of the heat source, and finally to verify the model. Sharples and co-workers [10] developed detailed finite-element modeling of a matrix of relevant un-repaired and repaired weld configurations. The finite-element models were carried out aimed at providing general guidance on welding repairs. Development and validation of the finite-element models were undertaken by way of an experimental program involving mechanical testing. Katsas et al. [11] examined the microstructural changes accompanying repair welding at the shipyards. The aluminum alloy 5083 was welded with a multi-pass sequence using the Metal Inert Gas (MIG) technique. After welding or during service, the defects were detected close to the weldment and then repairs were employed to extend the service life. Aloraier and co-workers [12] examined different percentages of bead overlaps and studied effects of Temper Bead Welding (TBW) on the mechanical properties as well as the microstructures. The results showed that desirable microstructures and hardness values could be obtained using flux cored arc welding when 70% bead overlap was used. Liu et al. [13] examined and quantified the effects of repeated repair cycles of TA15 titanium alloy plates on the microstructure features, elemental distribution, phase composition and mechanical properties. The results showed with increasing repair cycles the amount of the acicular α-phase in the weld seam increased; the size became larger and the alloy elements were distributed more unevenly between the weld seam and base metal. Furthermore, the hardness and fatigue properties of the joints decreased with increasing repair cycles, especially for the joint after the fourth welding repair. Vega and co-workers [14] presented the results of multiple weld repairs in seamless API X-52 micro alloyed steel pipe. The results indicated that relevant changes were not generated in the microstructural constituents of the HAZ. Moreover, significant reduction in Charpy-V impact resistance with the number of weld repairs was found when the notch location was in the intersection of the fusion line with the specimen mid-thickness. Branza et al. [15] perused the multi-pass weld-repair of heat-resistant cast steels that was carried out using an automated Shielded Metal Arc Welding (SMAW) process, with various filler materials and pre-heating at 400°C. It was concluded that even though buttering prevented cracking efficiently during welding, it was not acceptable as far as fatigue performance, especially lifetime, was concerned. Nascimento and co-worker [16] analyzed the effects of TIG welding repair on the structural integrity of the AISI 4130 aeronautical steel by experimental fatigue crack growth tests in base material, HAZ and weld metal. Increase of the fracture resistance was observed in the weld metal but decreasing in the HAZ after repair. The results were associated to micro hardness and microstructural changes with the welding sequence. Li and Shen [17] surveyed the single-pass friction stir weld of aluminum 2219-T6 with weld-defects repaired by overlapping friction stir welding technique. It was found that the phenomena of unusual particle-coarsening of Al_2Cu had occurred in the overlapping friction stir repair welds. The combined action of the three detailed mechanisms, including aggregation mechanism, diffusion mechanisms I and II contributed to the unusual coarsening behavior of Al_2Cu particles in the friction stir repair weld. Divya et al. [18] studied the importance of choosing suitable temperatures for two stages Post Weld Heat Treatment (PWHT) to achieve desirable toughness in the weld metals produced by ER 410NiMo filler wire. Results indicated by choosing appropriate temperatures for the PWHT, it is possible to obtain toughness in the weld metal, which was comparable to the toughness reported for the base metal of similar composition. Good toughness of the weld metal was attributed to the presence of retained austenite in the weld metal. Two stages of PWHT that gave excellent toughness for the weld metal was employed for repair of cracked shrouds of a steam turbine in a nuclear power plant. Lin et al. [19] investigated the effects of repeated weld-repairs on the microstructural and mechanical properties of AISI 304L stainless steel. In preparing the specimens, the root weld was fabricated using Gas Tungsten Arc Welding (GTAW). The weld bead was then ground away, and the weld was repaired using Shielded Metal Arc Welding (SMAW). The results showed that the microstructures of all specimens comprised a Body Centered Cubic (BCC) solid solution austenite matrix with interspersed ferrite phrase, and the fraction of low angle grain boundaries decreased with an increasing number of weld repairs. Moreover, the impact test results showed that the number of weld-repairs had no significant effect on the impact strength of the specimens, but affected the fracture characteristics. Azar and co-workers [20] looked at a selection of chamber gas composition for a viable and time-consuming underwater repair operation. Tensile and fracture toughness tests were performed on five bead-on-plate test samples that were welded under different chamber gas environments at 10 bars. The chemical composition, microstructure and mechanical properties of the weld metal were investigated. It was found that the pure *He* chamber gas offered the best visual and mechanical properties required by standards despite its high costs. Moreover, the properties of the weld metal using *Ar* and *Ar–He* mixtures were found to be slightly poorer than the properties in pure *He* case, yet better than the rest of the samples. Satheesh and Edwin [21] investigated an efficient technique to solve correlated multiple response optimization problems in the field of flux cored arc welding. This technique allows manufactures to develop intelligent manufacturing and repairing systems to achieve the highest level of automation.

In the present work yield stress, hardness and microstructures of the specimens were investigated before and after butt welding repair using the experimental study. The low-carbon steel A 36 thin plate was used to construct the specimens. This material has numerous applications to manufacture various structures and parts such as bridges, steel structures, auto parts and industrial machine components. The specifications of specimens and tests were selected according to American Welding Society (AWS) and American Society for Testing and Materials (ASTM) standards. The results included variation of the yield stress, the hardness and the microstructure occurred in the specimens after the welding repair.

2. SPECIFICATION OF THE SPECIMENS

Two A 36 plates with the dimension of 300 mm in length, 150 mm in width and 3 mm in thickness were butt welded by the Gas Tungsten Arc Welding (GTAW) method without using filler. The specifications of both initial and repair welds were selected according to AWS.D.1 standard. The combination of 75% *Ar* and 25% CO_2 was used as shield gas. According to the standard, single pass welding was applied for joining the two plates. The chemical composition of the used material and standard low carbon steel with the grade ASTM: A36 [22] are shown in Table 1. After welding, the specimens were cut from the welded plates using the Water Jet (WJ) method for avoiding heat effect during the cutting. The dimensional specifications of specimens were selected corresponding to AWS.B.4 [22]. The layout of the specimens before cutting and the detail of standard specimens are shown in Fig. 1.

Table 1. Chemical composition of the used material and low carbon steel with grade ASTM: A36 [22]

Grade	**Fe**	**C**	**Mn**	**Si**	**P**	**S**
Plate material	Base	0.140	0.910	0.160	0.002	0.005
ASTM: A 36	Base	0.100-0.300	0.500-1.000	0.100-0.250	0.040<	0.060<

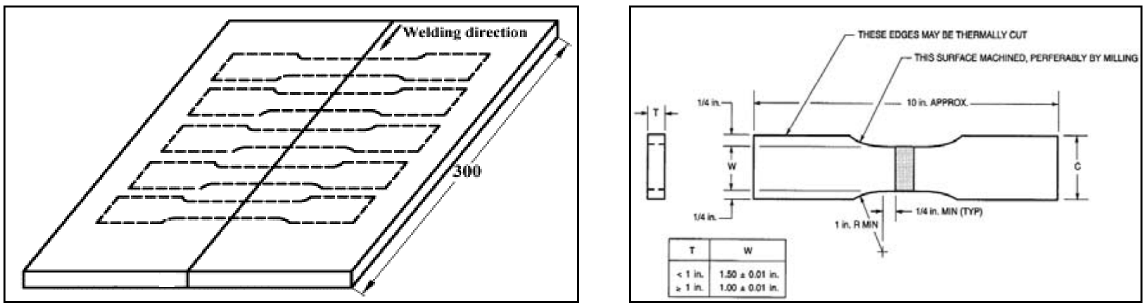

(a) (b)

Fig. 1. (a) The layout of the specimens before of cutting, (b) The detail of the standard specimens [22]

Four specimens using 15 V and 130 A and four specimens using 20 V and 150 A as operation conditions during initial welding of the plates were prepared. For readying the specimens including repair weld, first, original weld on the plates was machined through half- thickness of it by the shaper with strewing cooling fluid and then the plates were welded again with similar conditions with the initial welding. Thus, the eight specimens including repair welds in the two operation conditions were readied.

3. RESULTS OF TENSILE TESTS

The prepared specimens were exposed to tensile tests by a 60 kN servo-hydraulic INSTRON testing machine with strain rate, which was adjusted on 2 mm/min. Some specimens are shown after the tensile tests in Fig. 2.

According to Hall- Petch equation [23] by decreasing grin size in the microstructures the yield stress was increased. The grain size in base metal is coarser than in HAZ [24]. Therefore, the base metal in weldment reached yield condition sooner with respect to the HAZ. This matter can be observed from the results of the tests. All the specimens achieved failure in base metal and the distance about 20 mm from weld line. Figure 3 shows the fracture location in the specimen schematically.

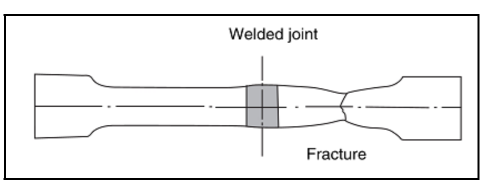

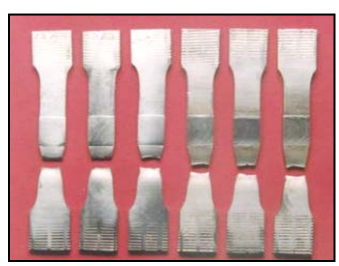

Fig. 2. Some Specimens after the tensile tests

Fig. 3. The fracture location in the specimen

Figure 4 shows the mean of yield stresses in the specimens was extracted using results of tests for both the specimens including initial and repair welds in 15 V and 130 A as welding conditions. The weld repair caused the mean of yield stresses in the specimens to reduce, although this reduction is small, in other words, the mean of yield stresses was changed from 330 MPa to 295 MPa by the repairing. The microstructures in HAZ were changed after the repairing as the grain size and width of HAZ were increased; hence the yield stress was decreased.

The values of yield stress mean were compared for the two repair conditions in Fig. 5. With increasing in the welding current and voltage the heat flux to welding zone was increased; therefore, the cooling rate was decreased and the grain size and width of HAZ were grown [25]. Thus, the mean of yield stress was decreased when the welding voltage and current increased.

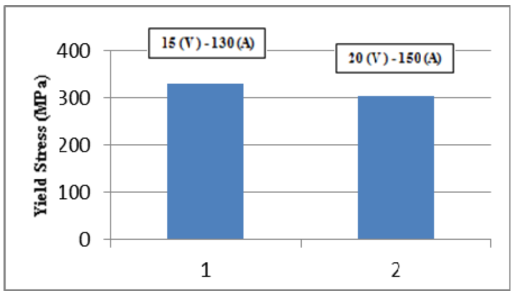

Fig. 4. The mean of yield stresses for the specimens

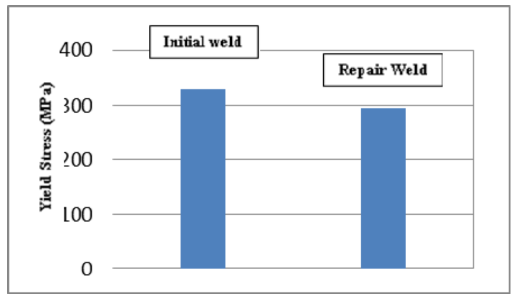

Fig. 5. Comparison the mean of yield stresses

4. RESULTS OF MICRO HARDNESS TESTS

The results of micro hardness tests of the specimens including initial and repair welds are shown in Fig. 6. In the base metal zone, the hardness after repairing was greater than before repairing, but in HAZ this matter was reverse. The grain size in HAZ would be coarse by doing the weld repair because the microstructures obtained another heat flux by the repairing; therefore, the hardness in HAZ would be decreased after repairing.

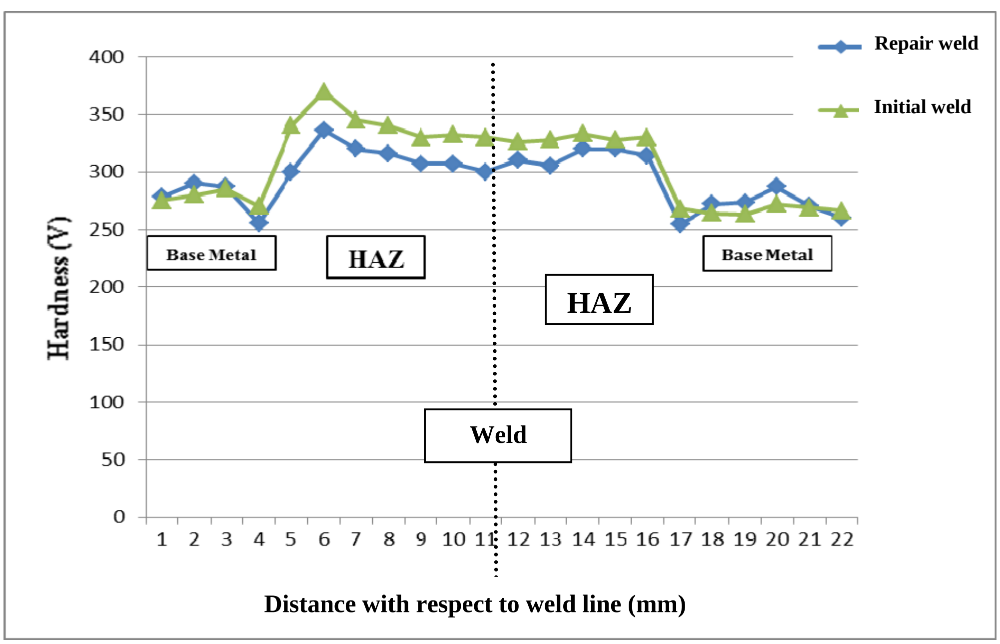

Fig. 6. Comparison of the surface hardness before and after welding repair

5. RESULTS OF MICROSTRUCTURES SCANS

For observation of the microstructures in the boundary between base metal and HAZ using Scanning Electron Microscope (SEM), first a sample with 15 mm diameter was cut from each specimen including initial and repair weld. The samples were polished and then etched by 4 % chloride acid. The SEM image of the sample before welding repair is shown in Fig. 7. This microstructure contained the pearlite. It corresponds to the description in Ref. [26]. The microstructure after the repair is shown in Fig. 8. In this image, the coarse-grained α ferrite, the pearlite and Widmanstatten ferrite structures are seen, which also correspond to Ref. [26]. To create ferrite phase and grow grain size caused a reduction of yield stress in the specimen which included welding repair. In Fig. 8, the martensite phase was not clearly seen in the microstructures. The specimen material was the low-carbon steel A 36; therefore, creation of martensite after repair was negligible [26].

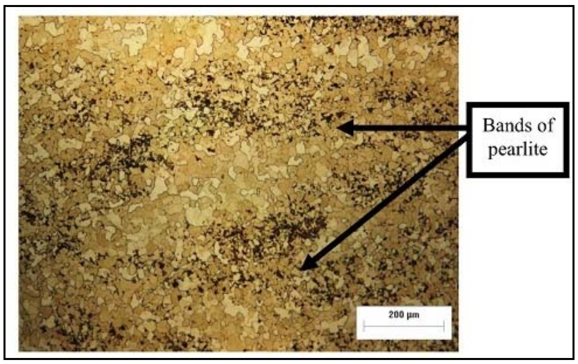

Fig. 7. The pearlite microstructure in the boundary between base metal and HAZ before weld repair

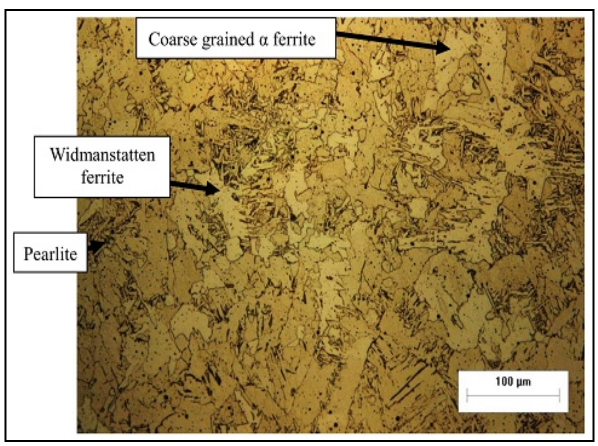

Fig. 8. The coarse-grained α ferrite, the pearlite and Widmanstatten ferrite microstructures in the boundary between base metal and HAZ after weld repair

6. CONCLUSION

The outcomes were obtained from the experimental study on the yield stress, hardness and microstructures of the specimens before and after butt welding repair consisted of the following results:

1. The mean of yield stresses in the specimens would be reduced after the repair through half-thickness of the butt weld, because grain size in the microstructures and width of HAZ were increased.

2. The mean of yield stresses in the specimens after repair would be decreased if the welding voltage and current increased, because the heat flux to welding zone was increased. It caused a decrease in the cooling rate and both the grain size and width of HAZ to increase.
3. The grain size in HAZ would be coarse by applying another heat flux during the weld repair; therefore, the hardness in HAZ would be decreased after repairing. In the base metal zone, the hardness after repairing was greater than it was before repairing, because the heat flux partially affected it.
4. The microstructure contained the pearlite phase before welding repair according to the SEM image of the sample. It is one of the reasons for the greater yield stress in the specimen including the initial weld with respect to the specimen after repairing.
5. The specimen that included repairing to weld had microstructures comprised of the coarse-grained α ferrite, the pearlite and Widmanstatten ferrite structures were seen from SEM image. The reduction of yield stresses in the specimens after repairing may be the result of creating the ferrite phase and increasing to the grain size.
6. The martensite phase was not clearly visible in the microstructure after repair, because the material used for constructing the specimens was the low-carbon steel.

REFERENCES

1. Kanne, Jr. W. R., Lohmeier, D. A., Dunn, K. A. & Tosten, M. H. (1993). Metallographic analysis of helium-embrittlement cracking of repair welds in nuclear reactor tanks. *Materials Characterization*, Vol. 30, No. 1, pp. 23-34.
2. Ghosh Chowdhury, S., Mukhopadhyay, N. K., Das, G., Das, S. K. & Bhattacharya, D. K. (1998). Failure analysis of a weld repaired steam turbine casing. *Engineering Failure Analysis*, Vol. 5, No. 3, pp. 205-18.
3. Kanne, Jr. W. R., Louthan, Jr. M. R., Rankin, D. T. & Tosten, M. H. (1999). Weld Repair of Irradiated Materials. *Materials Characterization*, Vol. 43, No. 2-3, pp. 203-14.
4. Lant, T., Robinson, D. L., Spafford, B. & Storesund, J. (2001). Review of weld repair procedures for low alloy steels designed to minimize the risk of future cracking. *International Journal of Pressure Vessels and Piping 2001*, Vol. 78, No. 11-12, pp. 813-18.
5. Otegui, J. L., Rivas, A., Manfredi, C. & Martins, C. (2001). Weld failures in sleeve reinforcements of pipelines. *Engineering Failure Analysis*, Vol. 8, No. 1, pp. 57-73.
6. Nonaka, I., Ito, T., Ohtsuki, S. & Takagi, Y. (2001). Performance of repair welds on aged 2.25Cr–1Mo boiler header welds. *International Journal of Pressure Vessels and Piping*, Vol. 78, No. 11-12, pp. 807-11.
7. Qian, M. & Lippold, J. C. (2003). The effect of rejuvenation heat treatments on the repair weldability of wrought Alloy 718. *Materials Science and Engineering: A*, Vol. 340, No. 1-2, pp. 225-31.
8. Branza, T., Duchosal, A., Fras, G., Deschaux-Beaume, F. & Lours, P. (2004). Experimental and numerical investigation of the weld repair of superplastic forming dies. *Journal of Materials Processing Technology*, No. 155-156, Vol. 1673-80.
9. Klobčar, D., Tušek, J. & Taljat, B. (2004). Finite element modeling of GTA weld surfacing applied to hot-work tooling. *Computational Materials Science*, Vol. 31, No. 3-4, pp. 368-78.
10. Sharples, J. K., Gardner, L., Bate, S. K., Goldthorpe, M. R., Yates, J. R. & Bainbridge, H. (2005). Project to evaluate the integrity of repaired welds. *International Journal of Pressure Vessels and Piping*, Vol. 82, No. 4, pp. 319-38.
11. Katsas, S., Nikolaou, J. & Papadimitriou, G. (2006). Microstructural changes accompanying repair welding in 5xxx aluminum alloys and their effect on the mechanical properties. *Materials & Design* Vol. 27, No. 10, pp. 968-75.

12. Aloraier, A., Ibrahim, R. & Thomson, P. (2006). FCAW process to avoid the use of post weld heat treatment. *International Journal of Pressure Vessels and Piping*, Vol. 83, No. 5, pp. 394-98.
13. Liu, L., Du, X., Zhu, M. & Chen, G. (2007). Research on the microstructure and properties of weld repairs in TA15 titanium alloy. *Materials Science and Engineering: A*, No. 445-446, Vol. 691-96.
14. Vega, O. E., Hallen, J. M., Villagomez, A. & Contreras, A. (2008). Effect of multiple repairs in girth welds of pipelines on the mechanical properties. *Materials Characterization*, Vol. 59, No. 10, pp. 1498-507.
15. Branza, T., Deschaux-Beaume, F., Velay, V. & Lours, P. (2009). A microstructural and low-cycle fatigue investigation of weld-repaired heat-resistant cast steels. *Journal of Materials Processing Technology*, Vol. 209, No. 2, pp. 944-53.
16. Nascimento, M. P. & Voorwald, H. J. C. (2010). Considerations about the welding repair effects on the structural integrity of an airframe critical to the flight-safety. *Procedia Engineering*, Vol. 2, No. 1, pp. 1895-903.
17. Li, B. & Shen, Y. (2011). The investigation of abnormal particle-coarsening phenomena in friction stir repair weld of 2219- T6 aluminum alloy. *Materials & Design*, Vol. 32, No. 7, pp. 3796-802.
18. Divya, M., Das, C. R., Ramasubbu, V., Albert, S. K. & Bhaduri, A. K. (2011). Improving 410NiMo weld metal toughness by PWHT. *Journal of Materials Processing Technology*, Vol. 211, No. 12, pp. 2032-38.
19. Lin, C. M., Tsai, H. L., Cheng, C. D. & Yang, C. (2012). Effect of repeated weld-repairs on microstructure, texture, impact properties and corrosion properties of AISI 304L stainless steel. *Engineering Failure Analysis*, Vol. 21, pp. 9-20.
20. Azar, A. S., Lange, H. I., Østby, E. & Akselsen, O. M. (2012). Effect of hyperbaric gas composition on mechanical properties of the weld metal. *Materials Science and Engineering: A*; In Press, Corrected Proof, Available online 9 July 2012.
21. Satheesh, M. & Edwin Raja Dhas J. (2013). Multi objective optimization of flux cored arc weld parameters using fuzzy based desirability function. *Iranian Journal of Science & Technology, Transactions of Mechanical Engineering*, Vol. 37, No. M2, pp. 175-187.
22. Structural welding code steel. (1996). American Welding Society (AWS).
23. Watt, D. F., Coon, L., Bibby, M., Goldak, J. & Henwood, C. (1988). An algorithm for modeling microstructural development in weld heat- affected zones: part A – reaction kinetics. *Acta Metal*, Vol. 36, No. 11, pp. 3029–35.
24. Varvara, R., Ruslan, B. & Siegfried, S. (2011). Three-dimensional analysis of mesoscale deformation phenomena in welded low-carbon steel. *Materials Science and Engineering: A*, Vol. 528, No. 15, pp. 5271-77.
25. Henwood, C., Bibby, M. J., Goldak, J. A. & Watt, D. F. (1988). Coupled transient heat transfer microstructure weld computations. *Acta Metal*, Vol. 36, No. 11, pp. 3037-46.
26. *Welding Handbook: Fundamentals of Welding*. (1976). 7th ed. American Welding Society.